Biosensors and Bioelectronics 87 (2017) 433–438

Contents lists available at ScienceDirect

Biosensors and Bioelectronics

journal homepage: www.elsevier.com/locate/bios

Surface plasmon resonance biosensor for sensitive detection of microRNA and cancer cell using multiple signal amplification strategy

Rongjuan Liu, Qing Wang *, Qing Li, Xiaohai Yang, Kemin Wang *, Wenyan Nie

State Key Laboratory of Chemo/Biosensing and Chemometrics, College of Chemistry and Chemical Engineering, Key Laboratory for Bio-Nanotechnology and Molecular Engineering of Hunan Province, Hunan University, Changsha 410082, China

ARTICLE INFO

Article history:
Received 14 June 2016
Received in revised form
25 August 2016
Accepted 26 August 2016
Available online 27 August 2016

Keywords:
Surface plasmon resonance
MicroRNA
Cancer cell
Gold nanoparticles
Silver nanoparticles
DNA supersandwich

ABSTRACT

A sensitive and versatile surface plasmon resonance (SPR) biosensor was proposed for the detection of microRNA (miRNA) and cancer cell based on multiple signal amplification strategy. Thiol-modified hairpin probe, including a sequence complementary to the target miRNA, was first immobilized on the Au film. In the presence of target miRNA, the stem-loop structure of hairpin probe was unfolded, and then DNA-linked Au nanoparticles (AuNPs) were hybridized with the terminus of the unfolded hairpin probe. Subsequently, DNA-linked AuNPs initiated the formation of DNA supersandwich structure through the addition of two report DNA sequences. Owing to the electronic coupling between localized plasmon of the AuNPs and the surface plasmon wave, as well as the enhancement of the refractive index of the medium over the Au film induced by DNA supersandwich structure, the SPR response was significantly enhanced. Next, numerous positively charged silver nanoparticles (AgNPs) were absorbed onto the long-range DNA surpersandwich equably, resulting in a further increase of SPR response. Due to the enzyme-free multiple signal amplification strategy, as low as ca. 0.6 fM miRNA-21 could be detected. In addition, this biosensor showed high selectivity toward single-base mismatch. More importantly, this SPR biosensor was also used for cancer cell detection coupled with the cell-specific aptamer modified magnetic nanoparticles. Given that the biosensor avoided enzyme introduction, the limitation of the enzyme was overcome. The versatile biosensor has great potential for the broad applications in the field of clinical analysis.

1. Introduction

Cancer is widely recognized as one of the serious diseases in modern society. Since the early diagnosis of cancer may be one of the feasible ways to diminish the cancer death-rate, it has received increasing attention in the field of cancer research. Since microRNAs (miRNAs), which are small non-coding regulatory RNAs (~22-nt) that regulate gene expression at the post-transcriptional level in the cytoplasm, have emerged as ideal noninvasive biomarkers candidates for early cancer diagnosis (Jeffrey, 2008), various sensing techniques, including electrochemical (Li et al., 2016b, 2016a; Rafiee-Pour et al., 2016), optical (Joshi et al., 2015; Liao et al., 2014; Qiu et al., 2015; Zhou et al., 2011) and mass-sensitive biosensors, etc. have been developed for sensitive and selective detection of miRNA. Due to the intrinsic properties of miRNAs, such as short size, low abundance, sequence similarity among family members and susceptibility to degradation, various amplifying strategies, including enzymatic signal amplification (Qiu et al., 2015), nanoparticle enhancement (Zhou et al., 2011) and strand displacement assay (Liao et al., 2014), have been developed for improving the detection sensitivity and adaptability. Besides miRNAs, cancer cells are also often detected with high selectivity and sensitivity in the field of cancer diagnosis (Chen et al., 2015; Gong et al., 2015; Jia et al., 2016; Savage, 2011; Sun et al., 2016; Wang et al., 2016c; Yu et al., 2016). To date, several cancer cell aptasensors have been explored, such as colorimetric method (Chen et al., 2015; Yu et al., 2016), fluorescence assay (Gong et al., 2015), surface plasmon resonance (SPR) (Jia et al., 2016), chemiluminescence biosensor (Wang et al., 2016c) and electrochemical biosensors (Sun et al., 2016). However, few literatures reported a versatile biosensor for the detection of miRNA and cancer cell (He et al., 2014).

Herein, a novel, sensitive and versatile SPR sensor was developed for miRNA and cancer cell based on multiple signal amplification strategy. The principle of this versatile biosensor was illustrated in Scheme 1. In the detection strategy, thiol-modified

* Corresponding authors.
E-mail addresses: wwqq99@hnu.edu.cn (Q. Wang), kmwang@hnu.edu.cn (K. Wang).

http://dx.doi.org/10.1016/j.bios.2016.08.090
0956-5663/

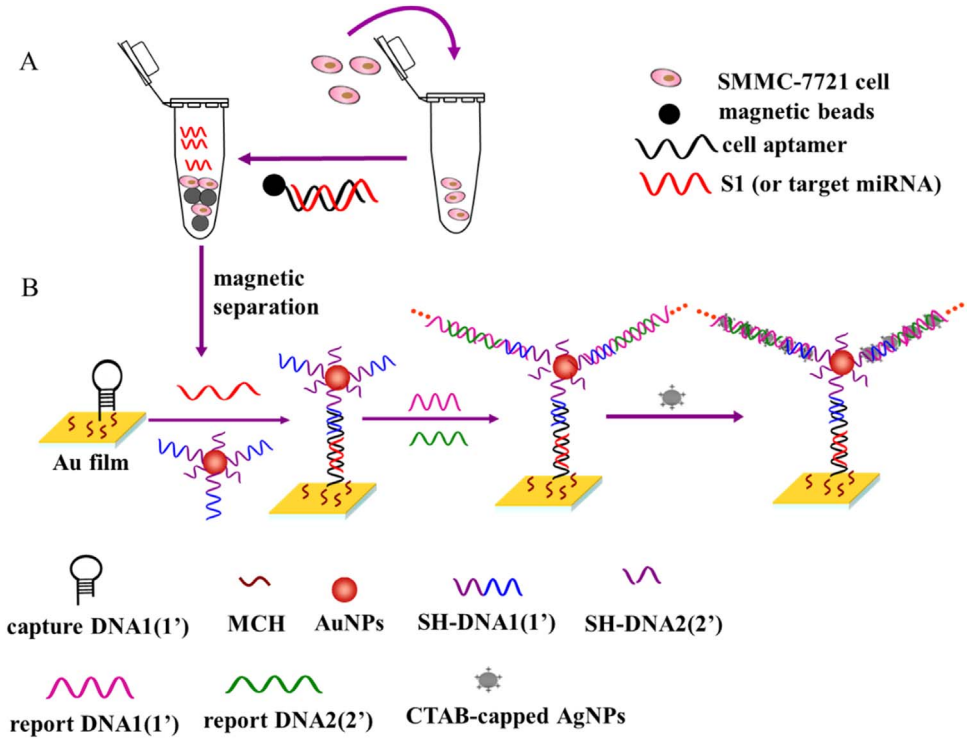

Scheme 1. Schematic representation of SPR biosensor based on multiple amplification strategy for miRNA and cancer cells detection.

hairpin probe including a sequence complementary to the target miRNA, was first immobilized on the Au film and used as capture DNA. In the presence of target miRNA, the stem-loop structure of capture DNA was unfolded, and then DNA-linked gold nanoparticles (AuNPs) were bound to Au film by hybridization with the terminus of capture DNA. Subsequently, DNA-linked AuNPs initiated the formation of DNA supersandwich structure as report DNA1 and report DNA2 were introduced. Due to the electronic coupling between localized plasmon of AuNPs and the surface plasmon wave associated with Au film, as well as the enhancement of the refractive index of the medium next to the Au film caused by DNA supersandwich structure, the shift of resonance angle was enhanced obviously. Next, numerous positively charged silver nanoparticles (AgNPs) were attached to the long-range negatively charged DNA surpersandwich, resulting in a further increase of resonance angle shift. According to the resonance angle shift, the concentration of target miRNA could be quantified.

More importantly, combined with the cell-specific aptamer and magnetic beads, the target cell could be detected using the above-mentioned biosensor. Briefly, cell aptamer modified magnetic beads were first hybridized with the S1 probe to form a duplex structure (shown in Scheme 1A). In the presence of target cell, aptamer immobilized on the magnetic beads could bind to the target cell, resulting in the release of S1 probe through magnetic separation. The released S1 probe, which was acted as the target nucleic acid, was then detected using the above mentioned SPR biosensor (shown in Scheme 1B). Subsequently, the target cell could be indirectly detected. The work demonstrated its potential application in early cancer diagnosis.

2. Experimental

2.1. Materials and reagents

Chloroauric acid ($HAuCl_4 \cdot 4H_2O$), trisodium citrate, silver nitrate ($AgNO_3$) and Sodium borohydride ($NaBH_4$) were purchased from Shanghai Reagent Company. (Shanghai, China). 6-Mercapto-1-hexanol (MCH) and hexadecyltrimethylammonium bromide (CTAB) were from Sigma (USA). Streptavidin-coated magnetic beads were obtained from Invitogen. Human hepatocarcinoma cell line Bel-7404, human normal liver cell line L-02 and human cervical carcinoma cell line Hela were purchased from Shanghai Institutes for Biological Science (China). Human hepatocellular carcinoma cell line SMMC-7721 was purchased from Xiangya School of Medicine, Central South University (China). The DNA sequences and ribonuclease (RNase) inhibitor were purchased from Shanghai Sangon Biotechnology Co. (Shanghai, China). All RNA sequences were synthesized by TaKaRa Biotechnology Co. (Dalian, China). The sequences of DNA and RNA were listed in Table 1. All other reagents used in the experiments were of analytical grade or higher. Ultrapure water (18.2 MΩ cm) was used throughout. Capture DNA and miRNA-21 were dissolved into 10 mM PBS buffer (pH 7.4) containing 300 mM NaCl. Report DNA1 and report DNA2 were dissolved into 20 mM Tris-HCl buffer (pH 7.4) containing 500 mM NaCl and 15 mM $MgCl_2$. For miRNA detection, all of the solutions were treated with diethylpyrocarbonate (DEPC) and autoclaved to protect from RNase degradation.

2.2. Preparation and modification of gold nanoparticles

AuNPs (~13 nm) were prepared by citrate reduction of $HAuCl_4$ (Frens, 1973). DNA-linked AuNPs were prepared according to our previous work (Wang et al., 2016b). Take DNA1 linked AuNPs as an example, assistant DNA1 (1 μM) and helper DNA (1 μM) were incubated with AuNPs solution at 4 °C for 16 h. Then, the solution was brought to 100 mM NaCl solution (pH 7.0, 10 mM phosphate buffer). After aging for 40 h at 4 °C, the DNA1-linked AuNPs were centrifuged at 13500g for 0.5 h to remove excess reagents. Then the red oily precipitate was washed twice with 100 mM NaCl solution (pH 7.0, 10 mM phosphate buffer) and then dispersed in 300 mM NaCl solution (pH 7.0, 10 mM phosphate buffer). AuNPs and DNA-linked AuNPs were respectively characterized using Uv–visible spectrophotometer (UV-1601, Shimadzu). The maximum

Table 1
Sequences of probes used.

Name	Sequence
Capture DNA1	5′-SH-C_6H_{12}-GGCCGTCAACATCAGTCTGATAAGCTAAACA TGATGACGGCC-3′
Capture DNA1′	5′-SH-C_6H_{12}-TTT TTG GGC GGG CGG TGC ATA GCG ACA CGC GCG CGC GCG CAC CTC AGC CAC CGC CCG CCC-3′
Assistant DNA1	5′-SH-C_6H_{12}-TTTTTGGCCGTCATCAT-3′
Assistant DNA1′	5′-SH-C_6H_{12}-TTTTTGGGCGGGCGGTG-3′
Helper DNA	5′-SH-C_6H_{12}-TTTTT-3′
Report DNA1	5′-TACTCCCCCAGGTGCATGATGACGGCC-3′
Report DNA2	5′-GCACCTGGGGGAGTAGGCCGTCATCAT-3′
Report DNA1′	5′-TACTCCCCCAGGTGCCACCGCCCGCCC-3′
Report DNA2′	5′-GCACCTGGGGGAGTAGGGCGGGCGGTG-3′
Aptamer	5′-biotin-ACG CGC GCG CGC ATA GCG CGC TGA GCT GAA GAT CGT ACC GTG AGC GCG T-3′
S1 probe	5′-GGTGCGCGCGCGCGTGTCGCT-3′
miRNA-21	5′-UAGCUUAUCAGACUGAUGUUGA-3′
Single base mismatch RNA (smRNA)	5′-UAGCUUAUCAG***U***CUGAUGUUGA-3′
Three base mismatch RNA (tmRNA)	5′-U***C***GCUUAUC***G***GACUGAU***C***UUGA-3′
Let-7c	5′-U***GAGG***UA***GU***AG***GU***UG***UAUGGUU***-3′
Let-7i	5′-U***GAGG***UA***GU***AG***UU***UG***UGCUGUU***-3′

*The bold, italic and underline bases are the mismatched bases.

absorption peak of unmodified AuNPs and DNA-linked AuNPs in solution were 518.0 nm and 524.0 nm, respectively (shown in Fig. S1 of the Supplementary material).

2.3. Preparation and characterization of silver nanoparticles (AgNPs)

AgNPs were prepared by reduction of $AgNO_3$ with $NaBH_4$ (Wei et al., 2005). In brief, 62.5 μM of CTAB ethanol solution was mixed with 4.69 mM of silver nitrate under vigorous stirring for 15 min. Then, the freshly prepared 1% $NaBH_4$ solution was added to the mixture drop wise until the color of the colloids became yellow green. Finally, AgNPs were characterized using Uv–visible spectrophotometer (UV-1601, Shimadzu) and Nano-ZS analyze (Malvern). The maximum absorption peak of AgNPs was recorded at 398.0 nm, and the zeta potential value of AgNPs was ca. +56 mV (shown in Fig. S2 of the Supplementary material).

2.4. Modification of magnetic beads using aptamer

Biotin-labeled SMCC-7721 cell specific aptamer (20 μL, 1 μM) was incubated with streptavidin-coated magnetic beads for 0.5 h at 37 °C. After magnetic separation, the above magnetic beads were rinsed three times with 1 × Tris buffer. Finally, the aptamer modified magnetic beads were dispersed in the Tris buffer.

2.5. Surface modification of Au film

Au film was first washed with acetone, ethanol and water for 2 min, respectively. Then the Au film was treated using fresh piranha solution (98% H_2SO_4/H_2O_2, 7:3 (v/v)) for 15–20 s, followed by a thorough rinsing with water. According to our previous work (Wang et al., 2016b), Au film was incubated with 5 μM capture DNA for 2 h. After rinsing with 10 mM PBS (pH 7.4) thoroughly, Au film was passivated with 1 mM MCH for 30 min to reduce nonspecific binding of DNA. In addition, thiol-modified capture DNA was also standing on the Au surface through the assembly of MCH (Herne and Tarlov, 1997). After thoroughly rinsing with 10 mM PBS, the sensor chip was obtained.

2.6. Detection of miRNA-21

All SPR measurements were performed with EC-SPR1010 device (Changchun Dingcheng Technology, China). Different concentrations of miRNA-21 solution were reacted with capture DNA1 immobilized on Au film for 50 min, then rinsed using 10 mM PBS repeatedly. Next, DNA1-linked AuNPs were injected and reacted for 1 h, followed by a thorough rinsing with 10 mM PBS. Then, a freshly prepared Tris-HCl buffer containing report DNA1 (4.5 μM) and report DNA2 (4.5 μM) was injected and incubated for 75 min, followed by a thorough washing with 10 mM PBS. Finally, AgNPs was incubated for 20 min. After the Au film was washed repeatedly with 10 mM PBS, the resonance angle was recorded. According to the shift of resonance angle after subtracting the response of the blank solution ($\Delta\theta$), the concentration of miRNA-21 could be determined. Here, 0.1% SDS/10 mM NaOH was used to regenerate the sensor chip for subsequent detection.

To identify the selectivity of this sensing system, different concentration solutions of miRNA-21, single-base mismatch RNA (smRNA), three-base mismatch RNA (tmRNA), let-7c and let-7i were respectively reacted with capture DNA1 which was modified on the Au film for 50 min at room temperature. After Au film was washed with 10 mM PBS thoroughly, the DNA1-linked AuNPs were added and reacted for 1 h. Next, the mixture of 4.5 μM report DNA1 and 4.5 μM report DNA2 was injected and incubated for 75 min at room temperature, followed by a thorough washing with 10 mM PBS. Finally, AgNPs was incubated for 20 min. After the Au film was washed using 10 mM PBS thoroughly, the resonance angle was recorded.

2.7. Analysis of SMMC-7721 cell

The SMMC-7721 cell aptamer modified magnetic beads were first hybridized with the complementary sequence (S1 probe, 0.1 μM) to form a duplex structure. Different concentrations of SMMC-7721 cell were incubated with the above solution for 30 min at 37 °C, and then magnetically separated. The released S1 probe in the supernatant, which was acted as the target, was detected using SPR biosensor based on multiple amplification strategy. The following processes were similar to the detection of miRNA-21. Similarly, different concentrations of other cells, such as L02 cell, Bel-7404 cell and Hela cell, were utilized as the control cell for identifying the selectivity of this sensing system.

3. Results and discussion

3.1. Investigation of the feasibility of SPR biosensor based on multiple amplification strategy

Take miRNA-21 for an example, the feasibility of the SPR biosensor was first investigated. As shown in Fig. 1, as 100 pM target miRNA-21 was incubated with capture DNA1 modified Au film, small resonance angle shift (0.0017°) was observed (from curve 1 to curve 2). Then DNA1-linked AuNPs were added, an obvious resonance angle shift (0.1075°) was obtained (from curve 2 to curve 3), implying that the DNA1-linked AuNPs were captured on the Au film through hybridization. Due to the electronic coupling between the localized plasmon of AuNPs and the surface plasmon wave associated with Au film, the SPR response was increased distinctly. After the report DNA1 and report DNA2 were injected, an obvious resonance angle shift (0.1689°) was obtained (from curve 3 to curve 4), suggesting that the DNA supersandwich structure was formed on the AuNPs modified Au film. Presumably, the refractive index of the medium adjacent to the Au film may be enhanced by DNA supersandwich products, resulting in the

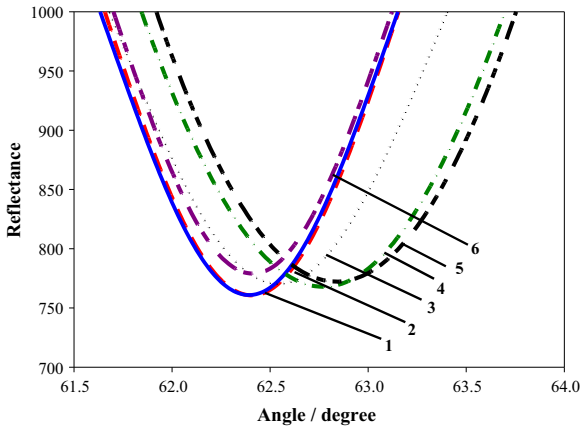

Fig. 1. SPR spectra of (1) capture DNA1 modified Au film; (2) hybridization with 100 pM miRNA-21; (3) reaction with the DNA1-linked AuNPs; (4) formation of DNA supersandwich on AuNPs; (5) absorption of AgNPs and (6) regeneration.

amplification of the SPR response. As AgNPs with positive charges were added, it resulted in the shift of the resonance angle shift (0.1076°) again (from curve 4 to curve 5). Apparently, the positively charged AgNPs were absorbed to the negatively charged DNA supersandwich through electrostatic adsorption. Subsequently, the SPR response was further enhanced. Moreover, when 0.1% SDS/10 mM NaOH was incubated for 5 min, SPR spectrum shifted from curve 5 to curve 6, and the resonance angle of curve 6 was basically consistent with that of curve 1, implying that regeneration of sensor chip was achieved by 0.1% SDS/10 mM NaOH. The results showed that miRNA-21 could be detected using SPR biosensor based on multiple amplification strategy.

3.2. Analytical performance of miRNA-21 detection

Different concentrations of miRNA-21 were then detected. Fig. 2A showed that the resonance angle gradually increased as the miRNA-21 concentration increased from 0 to 10 pM. It may be due to the increased quantity of AgNPs and DNA supersandwich modified AuNPs which were captured on Au film. Fig. 2B showed the relation between $\Delta\theta$ and the concentration of miRNA-21. It was estimated that the detection limit of the SPR biosensor based on multiple amplification strategy was 0.6 fM since a shift of resonance angle larger than 0.0015° was regarded as signal. Comparing with our previous work (Wang et al., 2016b), the detection limit of was ca. 1 order of magnitude lower than that of AuNPs coupling with supersandwich amplified SPR biosensor. That is to say, the detection limit was decreased more than 10 times by simply adding AgNPs. Moreover, the sensitivity of this sensor was comparable to or better than that of those previous works' (shown in Table 2), implying that the SPR biosensor based on multiple amplification strategy had high amplification efficiency.

The reproducibility of the sensor chip was then assessed. According to the results shown in Fig. 1, it was found that 0.1% SDS/10 mM NaOH could regenerate the sensor chip. As shown in Fig. 2C, almost no evidence of signal degradation was observed during the 6 cycles and the relative standard deviation (RSD) was 2.5% (n=6), suggesting that the reproducibility of the SPR biosensor was satisfactory. In view that participation of enzyme may induce irreversible damage to the architecture of miRNA biosensors, it is not easy to achieve reusable enzyme-amplified miRNA biosensor (Wang et al., 2015). Therefore, it was suggested that the present work was superior to those enzyme-based amplification assays in this regard.

For investigating the selectivity of the SPR biosensor, different concentration solutions of smRNA, tmRNA, let-7c and let-7i were respectively selected as contrasts. As shown in Fig. 2D, no measurable signal change for let-7c and let-7i was observed. Moreover, $\Delta\theta$ increased slightly with the increasing concentration of smRNA and tmRNA; while $\Delta\theta$ increased significantly with raising miRNA-21 concentration. It was suggested that this biosensor can distinguish miRNA-21 from smRNA.

Given that its high selectivity, the serum samples were also detected using such SPR biosensor. The human normal serum which did not contain miRNA in detectable quantity was first treated using the RNase inhibitor (Tran et al., 2013). Then different concentrations of miRNA-21 were introduced into the serum samples for obtaining miRNA-21 spiked serum samples. Next, after the miRNA-21 spiked serum samples were centrifuged to remove macromolecules (including HSA and other abundant proteins) using centrifugal filtration devices (10 K), such spiked serum samples were detected. As shown in Fig. 2E, the signal caused by miRNA-21 in human serum was similar to that in buffer, implying that the other components of the serum did not influence the measuring properties of the SPR sensor. The results demonstrated its potentials for practical applications.

3.3. Analytical performance of SMMC-7721 cell detection

Based on the specific recognition and high affinity of aptamer to cell, cancer cell was also detected using the above mentioned SPR biosensor. Here, human hepatoma SMMC-7721 cell was chosen as the model. As shown in Fig. 3A, the resonance angle increased with the increasing number of SMMC-7721 cells. Fig. 3B showed the relation between $\Delta\theta$ and the number of SMMC-7721 cell. A detection limit of 1 cell per μL could be estimated, which was comparable to or better than that of those previous works (Medley et al., 2008; Pan et al., 2009; Yin et al., 2013).

Different numbers of L-02 cell, Bel-7404 cell, and Hela cell were chosen as contrasts for investigating the selectivity of this system. As shown in Fig. 3C, $\Delta\theta$ increased slightly with increasing number of L-02 cells, Bel-7404 cells and Hela cells; while $\Delta\theta$ increased significantly with increasing number of SMMC-7721 cells. The results indicated that the biosensor has decent selectivity for SMMC-7721 cell detection.

In addition, SMMC-7721 cell in human serum was also detected using this biosensor. The samples were first obtained through adding SMMC-7721 cell in 20% serum. Then, the above samples were detected. As described in Fig. 3D, the SPR response resulted by SMMC-7721 cell in human serum was similar to that in buffer, implying that the SPR biosensor exhibited great potentials for practical applications.

4. Conclusion

In summary, a novel, enzyme-free and highly sensitive SPR biosensor based on multiple signal amplification strategy was introduced for detection of miRNA and cancer cell. Notwithstanding the complexity of the assay, the experimental operation was relatively robust, isothermal and cost-efficient. More importantly, the disadvantages of the use of enzyme were excluded since the assay avoided enzyme introduction. In addition, the assay offered high detection sensitivity and satisfactory selectivity. For practical application in disease diagnostics and clinical analyses, further attempts are underway to reduce the assay time and improve the convenience of procedures, such as introducing microfluidic technologies.

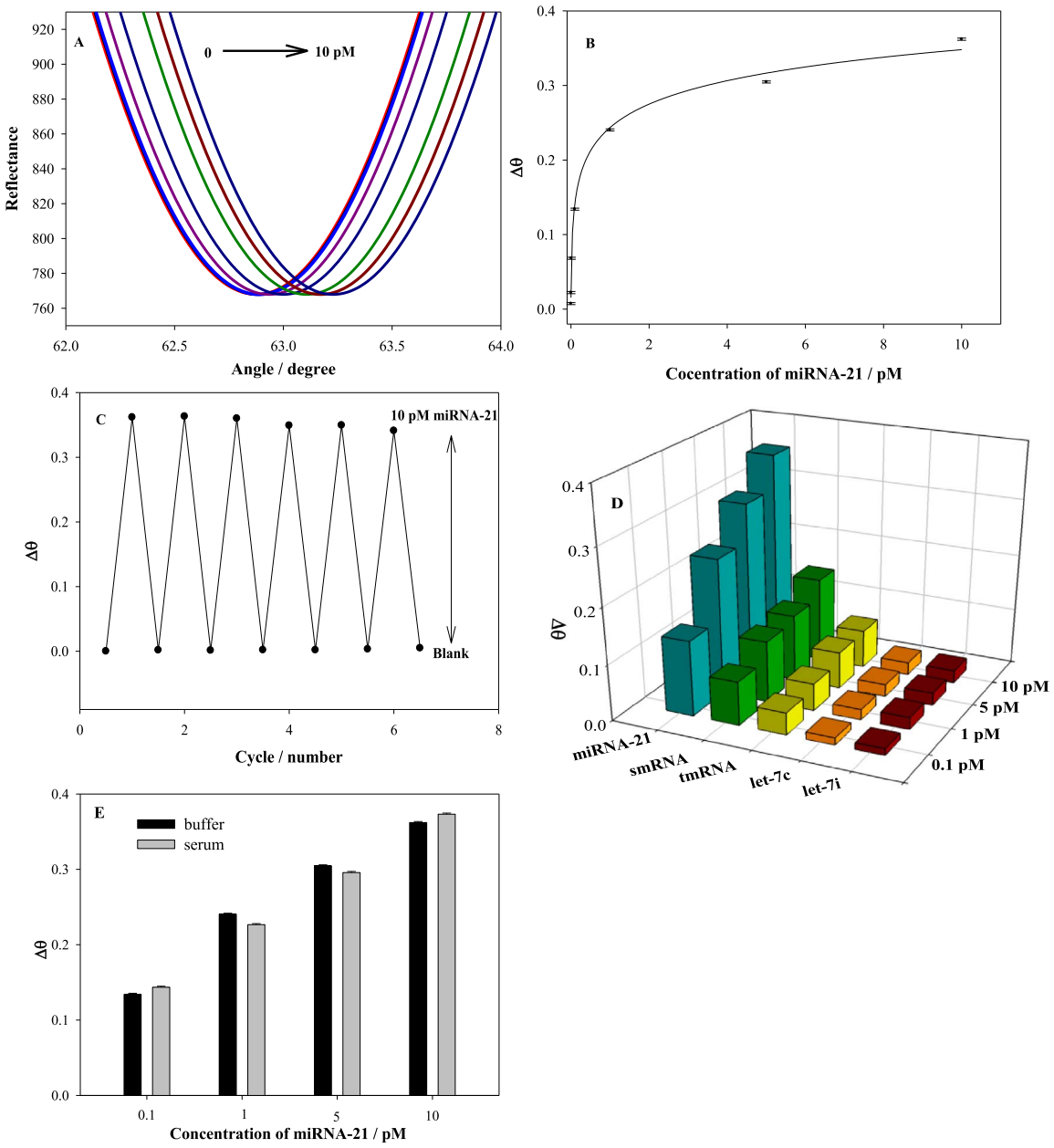

Fig. 2. (A) SPR spectra of different concentrations of miRNA-21. (B) The relationship between Δθ and miRNA-21 concentrations. (C) Reproducibility investigation of the SPR biosensor. The sensor chip was regenerated by introducing 0.1% SDS/10 mM NaOH for 5 min (D) Selectivity investigation of the SPR biosensor. (E) Detection of miRNA-21 in buffer and human serum. Δθ was the shift of resonance angle after subtracting the response of the blank solution. Error bars showed the standard deviation of measurement taken from three experiments.

Table 2
Detection performance comparison of our strategy versus other SPR biosensors.

SPR platform	Amplification strategy	Detection limit	Reference
SPR imaging	AuNPs amplification	0.5 pM	Vaisocherova et al. (2015)
SPRimager	silica nanoparticles and polymerase amplification	100 fM	Zhou et al. (2011)
SPRimager	AuNPs and polymerase amplification	10 fM	Fang et al. (2006)
Biacore X	streptavidin and supersandwich amplification	9 pM	Ding et al. (2015)
Biacore X	streptavidin and CHA amplification	1 pM	Li et al. (2016b)
SPR	AuNPs and DNA supersandwich amplification	8 fM	Wang et al. (2016b)
SPR	rGO and DSN amplification	3 fM	Qiu et al. (2015)
SPR	GO-AuNPs hybrids amplification	1 fM	Wang et al. (2016a)
SPR	multiple amplification strategy	0.6 fM	This work

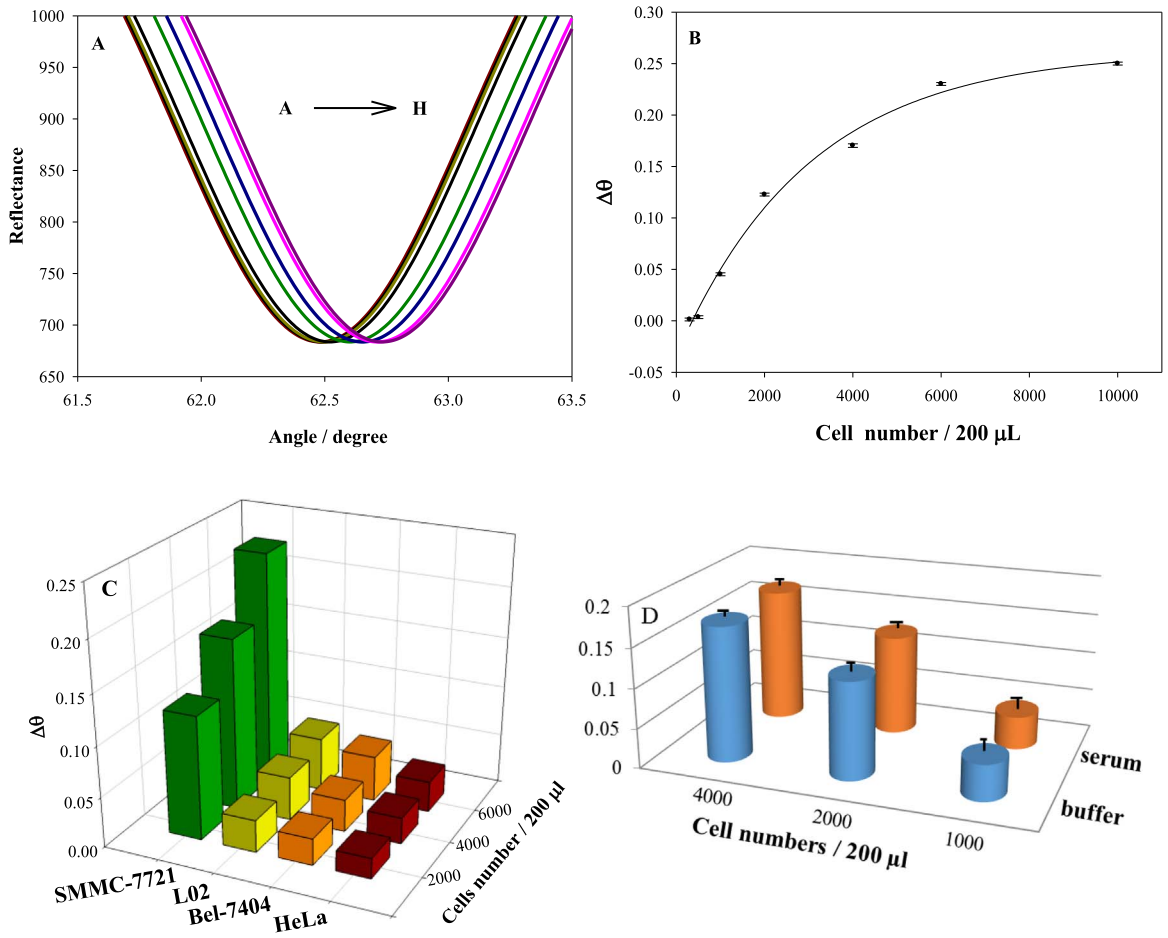

Fig. 3. (A) SPR spectra of different numbers of SMMC-7721 cell. From A to H: 200, 500, 1000, 2000, 4000, 6000 and 10,000 cells per 200 μL solutions. (B) The relationship between Δθ and SMMC-7721 cell numbers. (C) Selectivity investigation of the SPR biosensor. Δθ was the shift of resonance angle after subtracting the response of the blank solution. (D) Detection of SMMC-7721 cell in buffer and human serum. Error bars showed the standard deviation of measurement taken from three experiments.

Acknowledgments

This work was supported by the National Natural Science Foundation of China (21190040, 21375034 and 21175035) and Natural Science Foundation for Distinguished Young Scholars of Hunan Province for Distinguished Young Scholars of Hunan Province (2016JJ1008).

Appendix A. Supporting information

Supplementary data associated with this article can be found in the online version at http://dx.doi.org/10.1016/j.bios.2016.08.090.

References

Chen, C.H., Liu, Y.F., Zheng, Z.H., Zhou, G.H., Ji, X.H., Wang, H.Z., He, Z.K., 2015. Anal. Chim. Acta 880, 1–7.
Ding, X.J., Yan, Y.R., Li, S.Q., Zhang, Y., Cheng, W., Cheng, Q., Ding, S.J., 2015. Anal. Chim. Acta 874, 59–65.
Fang, S.P., Lee, H.J., Wark, A.W., Corn, R.M., 2006. J. Am. Chem. Soc. 128, 14044–14046.
Frens, G., 1973. Nat. Phys. Sci. 241, 20–22.
Gong, X., Zhou, W.J., Li, D.X., Chai, Y.Q., Xiang, Y., Yuan, R., 2015. Biosens. Bioelectron. 71, 98–102.
He, P., Qiao, W.P., Liu, L.J., Zhang, S.S., 2014. Chem. Commun. 50, 10718–10721.
Herne, T.M., Tarlov, M.J., 1997. J. Am. Chem. Soc. 119, 8916–8920.
Jeffrey, S.S., 2008. Nat. Biotechnol. 26, 400–401.
Jia, S.S., Li, P.F., Koh, K., Chen, H.X., 2016. Microchim. Acta 183, 683–688.
Joshi, G.K., Deitz-McElyea, S., Liyanage, T., Lawrence, K., Mali, S., Sardar, R., Korc, M., 2015. ACS Nano 9, 11075–11089.
Li, B.C., Liu, F., Peng, Y.Y., Zhou, Y.L., Fan, W.X., Yin, H.S., Ai, S.Y., Zhang, X.S., 2016. Biosens. Bioelectron. 79, 307–312.
Li, J.B., Lei, P.H., Ding, S.J., Zhang, Y., Yang, J.R., Cheng, Q., Yan, Y.R., 2016. Biosens. Bioelectron. 77, 435–441.
Liao, Y., Huang, R., Ma, Z., Wu, Y., Zhou, X., Xing, D., 2014. Anal. Chem. 86, 4596–4604.
Medley, C.D., Smith, J.E., Tang, Z.W., Wu, Y.R., Bamrungsap, S., Tan, W.H., 2008. Anal. Chem. 80, 1067–1072.
Pan, C.F., Guo, M.L., Nie, Z., Xiao, X.L., Yao, S.Z., 2009. Electroanalysis 21, 1321–1326.
Qiu, X.P., Liu, X., Zhang, W., Zhang, H., Jiang, T.L., Fan, D.L., Luo, Y., 2015. Anal. Chem. 87, 6303–6310.
Rafiee-Pour, H.-A., Behpour, M., Keshavarz, M., 2016. Biosens. Bioelectron. 77, 202–207.
Savage, N., 2011. Nature 471, S14–S15.
Sun, D.P., Lu, J., Zhong, Y.W., Yu, Y.Y., Wang, Y., Zhang, B.B., Chen, Z.G., 2016. Biosens. Bioelectron. 75, 301–307.
Tran, H.V., Piro, B., Reisberg, S., Tran, L.D., Duc, H.T., Pham, M.C., 2013. Biosens. Bioelectron. 49, 164–169.
Vaisocherova, H., Sipova, H., Visova, I., Bockova, M., Springer, T., Ermini, M.L., Song, X., Krejcik, Z., Chrastinova, L., Pastva, O., 2015. Biosens. Bioelectron. 70, 226–231.
Wang, Q., Li, Q., Yang, X.H., Wang, K.M., Du, S.S., Zhang, H., Nie, Y.J., 2016a. Biosens. Bioelectron. 77, 1001–1007.
Wang, Q., Liu, R.J., Yang, X.H., Wang, K.M., Zhu, J.Q., He, L.L., Li, Q., 2016b. Sens. Actuators B 223, 613–620.
Wang, Y.Z., Hao, N., Feng, Q.M., Shi, H.W., Xu, J.J., Chen, H.Y., 2016c. Biosens. Bioelectron. 77, 76–82.
Wang, Z.Y., Si, L., Bao, J.C., Dai, Z.H., 2015. Chem. Commun. 51, 6305–6307.
Wei, G., Wang, L., Liu, Z., Song, Y., Sun, L., Yang, T., Li, Z., 2005. J. Phys. Chem. B 109, 23941–23947.
Yin, J.J., He, X.X., Wang, K.M., Xu, F.Z., Shangguan, J.F., He, D.G., Shi, H., 2013. Anal. Chem. 85, 12011–12019.
Yu, T., Dai, P.P., Xu, J.J., Chen, H.Y., 2016. ACS Appl. Mater. Interfaces 8, 4434–4441.
Zhou, W.J., Chen, Y.L., Corn, R.M., 2011. Anal. Chem. 2011 (83), 3897–3902.